

Grain size and structure distortion characterization of α-MgAgSb thermoelectric material by powder diffraction

Xiyang Li(李西阳), Zhigang Zhang(张志刚), Lunhua He(何伦华), Maxim Avdeev, Yang Ren(任洋), Huaizhou Zhao(赵怀周), Fangwei Wang(王芳卫)

Citation: Chin. Phys. B . 2020, 29(10): 106101 . **doi:** 10.1088/1674-1056/aba09c
Journal homepage: http://cpb.iphy.ac.cn; http://iopscience.iop.org/cpb

What follows is a list of articles you may be interested in

Development of "Parameter space screening"-based single-wavelength anomalous diffraction phasing and structure determination pipeline

Wei Ding(丁玮), Xiao-Ting Wang(王小婷), Yang-Yang Yi(易阳旸)

Chin. Phys. B . 2019, 28(11): 116101 . **doi:** 10.1088/1674-1056/ab43bd

Isostructural phase transition-induced bulk modulus multiplication in dopant-stabilized ZrO_2 solid solution

Min Wang(王敏), Wen-Shu Shen(沈文舒), Xiao-Dong Li(李晓东), Yan-Chun Li(李延春), Guo-Zhao Zhang(张国召), Cai-Long Liu(刘才龙), Lin Zhao(赵琳), Shu-Peng Lv(吕舒鹏), Chun-Xiao Gao(高春晓), Yong-Hao Han(韩永昊)

Chin. Phys. B . 2019, 28(7): 076109 . **doi:** 10.1088/1674-1056/28/7/076109

Enhancement of MAD/MIR phasing at low resolution and a new procedure for automatic phase extension

Pu Han(韩普), Yuan-Xin Gu(古元新), Wei Ding(丁玮), Hai-Fu Fan(范海福)

Chin. Phys. B . 2019, 28(7): 076108 . **doi:** 10.1088/1674-1056/28/7/076108

Characterization of structural transitions and lattice dynamics of hybrid organic-inorganic perovskite $CH_3NH_3PbI_3$

Feng Jin(金峰), Jian-Ting Ji(籍建亭), Chao Xie(谢超), Yi-Meng Wang(王艺朦), Shu-Na He(贺淑娜), Lei Zhang(张磊), Zhao-Rong Yang(杨昭荣), Feng Yan(严锋), Qing-Ming Zhang(张清明)

Chin. Phys. B . 2019, 28(7): 076102 . **doi:** 10.1088/1674-1056/28/7/076102

Low temperature *Pmmm* and *C*2/*m* phases in $Sr_2CuO_{3+\delta}$ high temperature superconductor

Hai-Bo Wang(王海波), Zhen-Lin Luo(罗震林), Yuan-Jun Yang(杨远俊), Qing-Qing Liu(刘清青), Si-Xia Hu(胡思侠), Meng-Meng Yang(杨蒙蒙), Chang-Qing Jin(靳常青), Chen Gao(高琛)

Chin. Phys. B . 2019, 28(5): 056103 . **doi:** 10.1088/1674-1056/28/5/056103

Grain size and structure distortion characterization of α-MgAgSb thermoelectric material by powder diffraction*

Xiyang Li(李西阳)[1,2], Zhigang Zhang(张志刚)[1,3], Lunhua He(何伦华)[1,3], Maxim Avdeev[4], Yang Ren(任洋)[5], Huaizhou Zhao(赵怀周)[1], and Fangwei Wang(王芳卫)[1,2,3,†]

[1] *Beijing National Laboratory for Condensed Matter Physics, Institute of Physics, Chinese Academy of Sciences, Beijing* 100190, *China*
[2] *School of Physical Sciences, University of Chinese Academy of Sciences, Beijing* 101408, *China*
[3] *Songshan Lake Materials Laboratory, Dongguan* 523808, *China*
[4] *Australian Nuclear Science and Technology Organisation, Lucas Heights, NSW* 2234, *Australia*
[5] *X-ray Science Division, Argonne National Laboratory, Argonne, IL* 60439, *USA*

(Received 21 May 2020; revised manuscript received 18 June 2020; accepted manuscript online 29 June 2020)

Nanostructuring, structure distortion, and/or disorder are the main manipulation techniques to reduce the lattice thermal conductivity and improve the figure of merit of thermoelectric materials. A single-phase α-MgAgSb sample, $MgAg_{0.97}Sb_{0.99}$, with high thermoelectric performance in near room temperature region was synthesized through a high-energy ball milling with a hot-pressing method. Here, we report the average grain size of 24–28 nm and the accurate structure distortion, which are characterized by high-resolution neutron diffraction and synchrotron x-ray diffraction with Rietveld refinement data analysis. Both the small grain size and the structure distortion have a contribution to the low lattice thermal conductivity in $MgAg_{0.97}Sb_{0.99}$.

Keywords: diffraction, grain size, structure distortion, thermoelectric material

PACS: 61.05.cp, 61.05.fm, 84.60.Rb **DOI:** 10.1088/1674-1056/aba09c

1. Introduction

Thermoelectric materials, which can be used for interconversion of thermal energy and electrical energy based on the thermoelectric effect, are widely studied in thermoelectrical systems for cooling or heating, and regenerating electricity.[1,2] The energy conversion efficiency (η) can be calculated via[1]

$$\eta = \eta_{\text{Carnot}} \frac{\sqrt{1+ZT}-1}{\sqrt{1+ZT}+T_{\text{C}}/T_{\text{H}}}, \tag{1}$$

where η_{Carnot} is the Carnot cycle efficiency, T_{H} and T_{C} are the temperatures at the hot junction and the surface being cooled, and ZT is the figure of merit. $ZT = [S^2\sigma/(\kappa_{\text{lat}} + \kappa_{\text{ele}})]T$, where S, σ, κ_{lat}, κ_{ele}, and T are the Seebeck coefficient, electronic conductivity, lattice thermal conductivity, electronic thermal conductivity, and absolute temperature, respectively.[1] Thus, η is dominated by the ZT value in the situation with a given temperature difference.

One of the main methods to improve ZT is the nanocrystallization synthetic technique resulting in κ_{lat} suppression of phonon scattering from micro-nano scale boundaries and interfaces.[2–5] Poudel *et al.* developed a nanostructuring approach which significantly improved the ZT value of the thermoelectric material BiSbTe.[3] The sample was synthesized by a two-step ball milling and hot-pressing method. With high-resolution transmission electron microscopy (TEM), the grains of 2- to 10-nm-size with fuzzy boundaries were reported.[3] The improvement of ZT in BiSbTe nano-crystallization material mainly comes from the low κ_{lat}, caused by the phonon scattering from grain boundaries and defects.[3] Here, using this method,[3] we synthesized a single-phase $MgAg_{0.97}Sb_{0.99}$ sample,[6] a near room temperature high-performance α-MgAgSb thermoelectric material with low thermal conductivity.[6–10] Recently, the mechanism of the transverse acoustic phonon suppressed by the local structure distortion has been demonstrated by inelastic neutron scattering and *ab initio* calculations in α-MgAgSb.[11] Although it was believed to be a primary factor for the low thermal conductivity, the small grain size was proposed as another mechanism.[6,9] Our previous TEM results showed that their grains are smaller than 20 nm.[6] In contrast to TEM as a microscopical technique, the macroscopical characterization of grain size remains elusive.

Another main method to improve ZT is structure manipulation, such as structure disorder and/or distortion, including both dynamic and static structure defects.[1,11–14] The mechanisms of Ag atoms dynamic disorder induced low thermal conduction have been studied in superionic conductor MCr_2Se_2 (M = Cu, Ag) thermoelectric materials.[13,14] One of the most famous thermoelectric materials, SnSe with $ZT = 2.6$ and ultralow thermal conductivity of 0.23 $W\cdot m^{-1}\cdot K^{-1}$, mainly bene-

*Project supported by the National Natural Science Foundation of China (Grant No. 11675255) and the National Key R&D Program of China (Grant No. 2016YFA0401503).

†Corresponding author. E-mail: fwwang@iphy.ac.cn

© 2020 Chinese Physical Society and IOP Publishing Ltd

fits from its 3D distorted NaCl structure.[12] The local structure distortion in a Ni-doped sample of $MgAg_{0.965}Ni_{0.005}Sb_{0.99}$ has been studied by neutron total scattering with pair distribution function (PDF) analysis.[11] An accurate characterization of the structural distortion in $MgAg_{0.97}Sb_{0.99}$ remains elusive.

Here, we use high-resolution neutron diffraction and synchrotron x-ray diffraction to study the average grain size and the structure distortion in $MgAg_{0.97}Sb_{0.99}$ samples. By Rietveld refinement using FullProf suite,[15] we report that the average size of the grains in $MgAg_{0.97}Sb_{0.99}$ sample is 24–28 nm, relatively larger than the microscopic measurements, and the significant structure distortion of the Mg–Sb distorted NaCl structure characterized by bond distances and bond angles.

2. Experiments and methods

The sample synthesize method of $MgAg_{0.97}Sb_{0.99}$ has been reported elsewhere.[6]

The high-resolution neutron diffraction measurements were performed at room temperature (RT) using ECHIDNA[16] at the ANSTO, Australia. A Ge (335) monochromator was used to produce a monochromatic neutron beam of wavelength 1.6215(1) Å. The synchrotron x-ray diffraction measurements were carried out at RT at the 11-ID-C station, Advanced Photon Source, Argonne National Laboratory. High-energy x-rays with a wavelength of 0.117418 Å were used in transmission geometry.

In diffraction experiments, the smaller grain size makes diffraction Bragg peaks broader because of the broken of the sample's long-range periodicity.[17] Thus, the peak width contains the information of grain size. FullProf suite provides a method to calculate the average grain size for constant wavelength mode.[15] The refined parameters are related to the peak width. On another side, the refined bond distances and bond angles can be used to characterize the static structure distortion.

In FullProf suite,[15] Thompson–Cox–Hastings pseudo-Voigt convoluted with axial divergence asymmetry function ($Npr = 7$) is used for grain size refinement. The full width at half maximum (FWHM) of the Gaussian (H_G) and Lorentzian (H_L) components is calculated as

$$H_G^2 = \left(U + D_{ST}^2\right)\tan^2\theta + V\tan\theta + W + \frac{I_G}{\cos^2\theta}, \quad (2)$$

$$H_L = X\tan\theta + \frac{[Y + F(S_Z)]}{\cos\theta}, \quad (3)$$

where U, V, W, X, and Y are the refinement parameters and θ is half of the scattering angle 2θ.

The apparent grain size can be calculated by

$$D_h = \frac{\eta_s + (1-\eta_s)\sqrt{\pi \ln 2}}{Z_s}\left(\frac{360\lambda}{\pi^2}\right), \quad (4)$$

where λ is the wavelength of neutron or x-ray and

$$Z_s^5 = I_G^{5/2} + 2.69269 I_G^2 Y_L + 2.42843 I_G^{3/2} Y_L^2 + 4.47163 I_G Y_L^3 + 0.07842 I_G^{1/2} Y_L^4 + Y_L^5,$$

$$\eta_s = 1.36603\frac{Y_L}{Z_s} - 0.47719\left(\frac{Y_L}{Z_s}\right)^2 + 0.11116\left(\frac{Y_L}{Z_s}\right)^3.$$

In the size effect refinement of FullProf suite, the grain size parameters GausSiz and LorSiz are used, which are corresponding to I_G = GausSiz and $Y_L = Y$ + LorSiz in the above equations.

In the Rietveld refinement, we first deal with the scale factor, the diffractometer zero point factor, and the background function factors, then with the lattice parameters, the profile function parameters, the atomic coordinates, and the overall isotropic displacement factor, and finally with the size parameters.

3. Results and discussion

Figure 1(a) shows the crystal structure of α-MgAgSb (space group: I-4c2, No. 120), which is used as the original structure model of the refinement.[18] Figure 1(b) shows the raw high-resolution neutron and synchrotron x-ray diffraction patterns. Although the synchrotron x-ray diffraction has a higher resolution than neutron diffraction, it suffers from the form factor drop-off near the large Q side.[19]

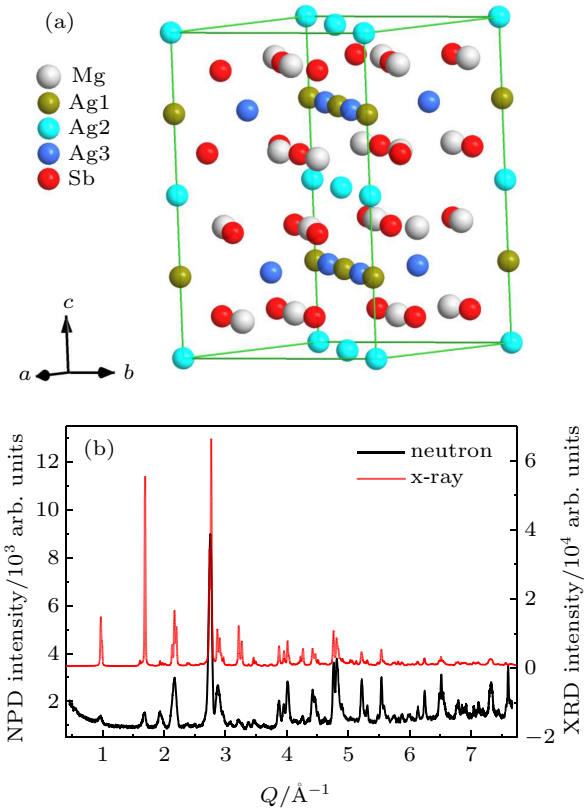


Fig. 1. (a) Crystalline structure of α-MgAgSb, the space group is I-4c2 (No. 120). (b) The neutron diffraction, and synchrotron x-ray diffraction data of $MgAg_{0.97}Sb_{0.99}$ measured at room temperature.

Table 1. Refined parameters of $MgAg_{0.97}Sb_{0.99}$ measured by high resolution neutron diffraction and synchrotron x-ray diffraction, respectively.

		Neutron diffraction	X-ray diffraction
Cell parameters:			
a, b/Å		9.1706(7)	9.1723(3)
c/Å		12.7082(9)	12.7100(4)
V/Å^3		1068.8(2)	1069.1(2)
Atom parameters:			
Mg	x	−0.0232(4)	−0.030(2)
	y	0.2837(4)	0.284(2)
	z	0.1101(3)	0.1128(9)
Ag1	x	0	0
	y	0	0
	z	0.25	0.25
Ag2	x	0	0
	y	0	0
	z	0	0
Ag3	x	0.2239(3)	0.2243(4)
	y	0.2239(3)	0.2243(4)
	z	0.25	0.25
Sb	x	0.2353(4)	0.2357(3)
	y	0.4751(4)	0.4767(3)
	z	0.1180(3)	0.1172(2)
Mg–Sb bond distances:			
b1/Å		2.937(5)	2.97(2)
b2/Å		2.948(4)	2.90(2)
b3/Å		2.952(4)	3.02(2)
b4/Å		3.247(4)	3.21(2)
b5/Å		3.460(5)	3.44(2)
b6/Å		3.871(4)	3.90(2)
Mg-Sb bond angles:			
b1–b2/(°)		100.2(3)	99.9(3)
b1–b3/(°)		87.0(2)	85.4(3)
b1–b4/(°)		95.2(2)	94.8(3)
b1–b6/(°)		83.1(2)	81.7(3)
b2–b3/(°)		94.7(2)	94.6(3)
b2–b4/(°)		95.6(2)	97.5(3)
b2–b5/(°)		90.0(2)	91.8(3)
b3–b5/(°)		90.0(2)	89.8(3)
b3–b6/(°)		83.5(2)	82.1(3)
b4–b5/(°)		86.0(2)	87.5(3)
b4–b6/(°)		86.0(2)	85.8(3)
b5–b6/(°)		86.6(2)	86.3(2)
X and Y parameters:			
X/(°)		–	0.36431
Y/(°)		0.184(6)	0.0012(2)
Size parameters:			
GausSiz/(°)^2		0.008(2)	0.000617(3)
Grain size/nm		28(4)	24(1)
Reliability factors[a]:			
R_{wp}/%		10.8	9.94
χ^2		1.98	10.2

[a]R_{wp}, weighted profile factor; χ^2, goodness of fit.

The refinement results of neutron diffraction data are shown in Fig. 2 and Table 1. Figure 2(a) shows the refinement pattern with the size parameter refined. Here, the refinement result is good enough using one size parameter of GausSiz. For comparison, the refinement result without the size parameter is shown in Fig. 2(b). With the size parameter refined, the reliability factors are apparently improved, such as R_{wp} from 12.8% to 10.8% and χ^2 from 2.53 to 1.98. As the size parameter changes the peak shape, the residual (blue lines in Fig. 2) improvement can be apparently seen, such as at the sharpest peak of $Q \sim 2.75$ Å^{-1} and another peak with a high scattering angle of $Q \sim 6.5$ Å^{-1}. The calculated grain size from the refined parameters is 28(4) nm, a little larger than our previous measurements by TEM, where it was smaller than 20 nm.[6]

To further verify the results, the synchrotron x-ray diffraction measurements were performed. Here, the same grain size refinement method with neutron diffraction data is used. The refinement results are shown in Fig. 3 and Table 1. Figure 3(a) shows the refinement pattern with the size parameter GausSiz refined. For comparison, the refinement result without the size parameter is shown in Fig. 3(b). After GausSiz is refined, the reliability factors are improved, such as R_{wp} from 10.2% to 9.94% and χ^2 from 10.7 to 10.2. Here, the calculated grain size from the refined parameters is 24(1) nm, just between the value of 28(4) nm by neutron diffraction and the value of 10–20 nm by TEM. We show that this macroscopical average grain size characterization method is powerful since it is complementary to the microscopical TEM measurements.

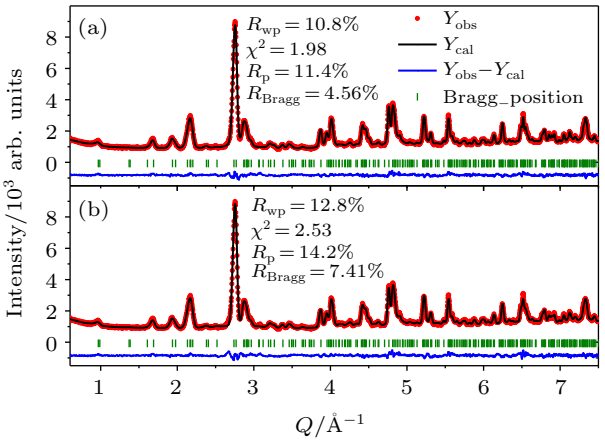


Fig. 2. Rietveld refinement of $MgAg_{0.97}Sb_{0.99}$ neutron diffraction data with size parameter refined (a), and without size parameter refined (b).

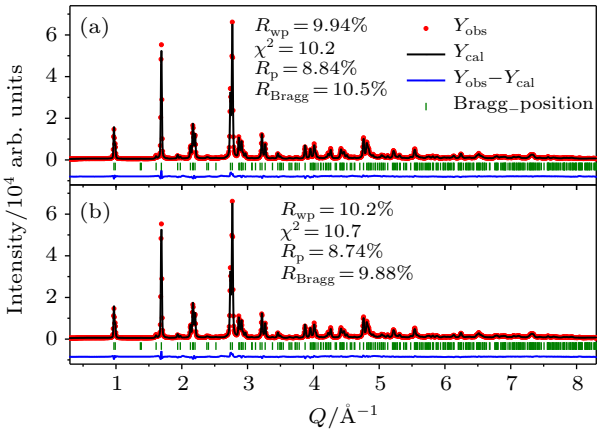


Fig. 3. Rietveld refinement of $MgAg_{0.97}Sb_{0.99}$ synchrotron x-ray diffraction data with size parameter refined (a), and without size parameter refined (b).

The static structure distortion is further studied by the analysis of the refined bond distances and bond angles. In α-MgAgSb, the Mg and Sb atoms form a three-dimensional distorted NaCl structure (Fig. 4). The refined nearest Mg–Sb bond distances and bond angles from the high-resolution neutron diffraction data and synchrotron x-ray diffraction data are shown in Table 1. In a nondistorted NaCl structure, the nearest bond distances should be equal and the corresponding bond angles are 90°. Here, the nearest Mg–Sb bond distances vary greatly, and the corresponding bond angles deviate from 90° (some of them even as large as 10° such as the angle of bonds b1–b2) which characterizes its heavy distortion feature. This structure distortion results in $MgAg_{0.97}Sb_{0.99}$ are consistent with our recent studying results where the neutron total scattering combined with PDF analysis was used to study the local structure distortion in $MgAg_{0.965}Ni_{0.005}Sb_{0.99}$.[11] By PDF analysis, the bond length distribution information of the Mg–Sb pairs was established.[11] There are three broad peaks located at $r \sim 2.9$ Å, 3.3 Å, and 3.8 Å, which are corresponding to the Rietveld refinement averaged results of Mg–Sb bond distances from 2.90(2) Å to 3.90(2) Å in this work (Table 1). As demonstrated in our recent work,[11] the structure distortion has a strong suppression on transverse phonons and results in ultralow lattice thermal conductivity in α-MgAgSb materials. Besides that, the small grain size with more boundaries and interfaces is another phonon scattering mechanism that leads to the ultralow thermal conductivity in α-MgAgSb materials.

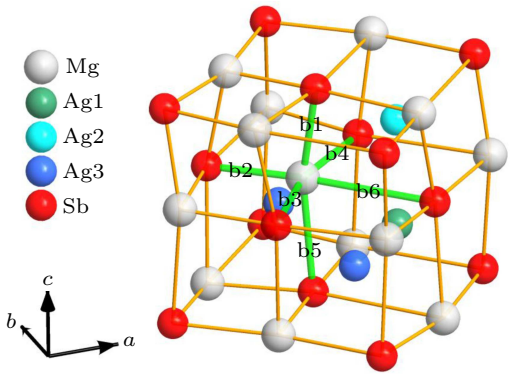


Fig. 4. Static structure distortion in $MgAg_{0.97}Sb_{0.99}$. The refined bond distances and bond angles of the nearest Mg–Sb bonds are shown in Table 1. The refinement results show a significant distortion of this Mg–Sb formed distorted NaCl structure.

4. Conclusion

The average grain size and static structure distortion of $MgAg_{0.97}Sb_{0.99}$ sample have been studied by high-resolution neutron diffraction and synchrotron x-ray diffraction with Rietveld refinement using FullProf suite. The grain size is 24–28 nm, comparatively larger than the upper value obtained by the TEM measurements, i.e., 20 nm. Even so, this difference is insignificant due to the difference between these two methods. The Mg–Sb atoms formed three-dimensional distorted NaCl structure has been accurately characterized by their bond distances and bond angles. The small grain size and structure distortion all contribute to the low thermal conductivity in $MgAg_{0.97}Sb_{0.99}$.

References

[1] Takabatake T, Suekuni K, Nakayama T and Kaneshita E 2014 *Rev. Mod. Phys.* **86** 669
[2] He J and Tritt T M 2017 *Science* **357** eaak9997
[3] Poudel B, Hao Q, Ma Y, Lan Y, Minnich A, Yu B, Yan X, Wang D, Muto A, Vashaee D, Chen X, Liu J, Dresselhaus M S, Chen G and Ren Z 2008 *Science* **320** 634
[4] Zhao H, Pokharel M, Chen S, Liao B, Lukas K, Opeil C, Chen G and Ren Z 2012 *Nanotechnology* **23** 505402
[5] Du B S, Jian J K, Liu H T, Liu J and Qiu L 2018 *Chin. Phys. B* **27** 048102
[6] Zhao H, Sui J, Tang Z, Lan Y, Jie Q, Kraemer D, McEnaney K, Guloy A, Chen G and Ren Z 2014 *Nano Energy* **7** 97
[7] Li D, Zhao H, Li S, Wei B, Shuai J, Shi C, Xi X, Sun P, Meng S, Gu L, Ren Z and Chen X 2015 *Adv. Funct. Mater.* **25** 6478
[8] Liu Z, Wang Y, Mao J, Geng H, Shuai J, Wang Y, He R, Cai W, Sui J and Ren Z 2016 *Adv. Energy Mater.* **6** 1502269
[9] Liu Z, Mao J, Sui J and Ren Z 2018 *Energy Environ. Sci.* **11** 23
[10] Wang J F, Fu X N, Zhang X D, Wang J T, Li X D and Jiang Z Y 2016 *Chin. Phys. B* **25** 086302
[11] Li X, Liu P, Zhao E, Zhang Z, Guidi T, Le M D, Avdeev M, Ikeda K, Otomo T, Kofu M, Nakajima K, Chen J, He L, Ren Y, Wang X L, Wang B T, Ren Z, Zhao H and Wang F 2020 *Nat. Commun.* **11** 942
[12] Zhao L D, Lo S H, Zhang Y, Sun H, Tan G, Uher C, Wolverton C, Dravid V P and Kanatzidis M G 2014 *Nature* **508** 373
[13] Li B, Wang H, Kawakita Y, Zhang Q, Feygenson M, Yu H L, Wu D, Ohara K, Kikuchi T, Shibata K, Yamada T, Ning X K, Chen Y, He J Q, Vaknin D, Wu R Q, Nakajima K and Kanatzidis M G 2018 *Nat. Mater.* **17** 226
[14] Niedziela J L, Bansal D, May A F, Ding J, Lanigan-Atkins T, Ehlers G, Abernathy D L, Said A and Delaire O 2019 *Nat. Phys.* **15** 73
[15] Rodríguez-Carvajal J 1993 *Physica B* **192** 55
[16] Avdeev M and Hester J R 2018 *J. Appl. Crystallogr.* **51** 1597
[17] Scheer A, Kruppke H and Heib R 2004 *Diffraction Analysis of the Microstructure of Materials* Vol. 68 (Berlin, Heidelberg: Springer)
[18] Kirkham M J, dos Santos A M, Rawn C J, Lara-Curzio E, Sharp J W and Thompson A J 2012 *Phys. Rev. B* **85** 144120
[19] Cardona M and Merlin R 2006 *Light Scattering in Solid IX* Vol. 108 (Berlin, Heidelberg: Springer)